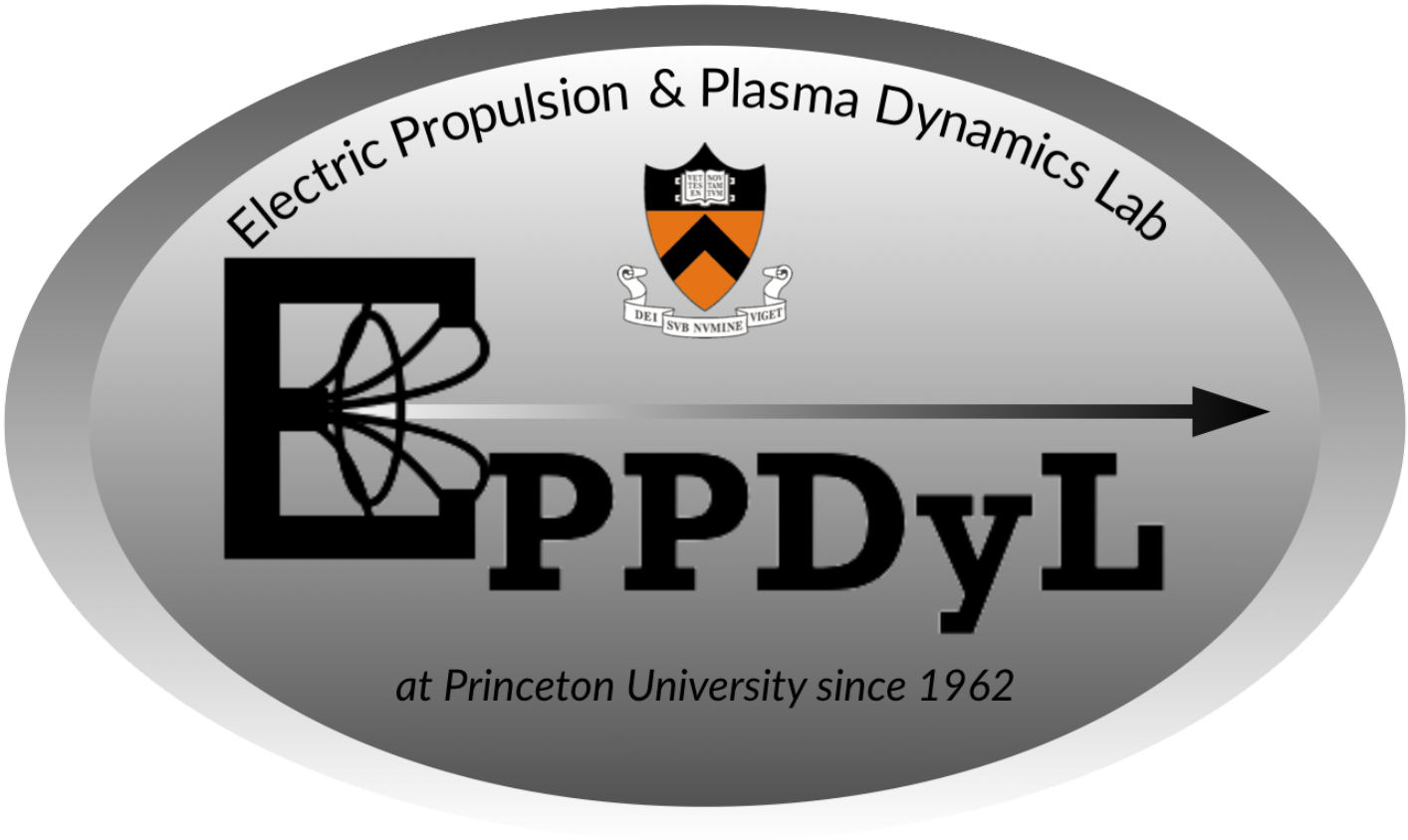

Lorentz Force Accelerators (LFAs)

Research supported by:

- NASA-JPL's Advanced Propulsion Group, and

- the Princeton Plasma Physics Laboratory's Program in Plasma Science and Technology (http://w3.pppl.gov/ppst/)

Motivation

The promise of achieving high thrust density coupled with high specific impulse is the motivation behind research into the lithium and argon Lorentz force accelerators (LiLFA and ALFA respectively). The combination of these thruster characteristics enables the cost saving benefits of electric propulsion to be applied to missions requiring short transit times, such as manned missions to Mars and beyond. The LFA provides a higher thrust density than any currently flying electric propulsion device and is realistically only limited in thrust by the amount of available power.

In one sentence: We want to send people to Mars, but we don't want to spend a lot of money.

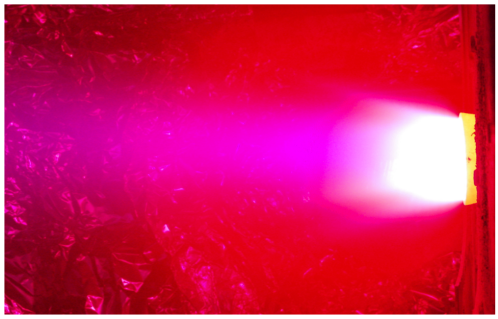

Figure 1 - The LiLFA firing on May 7, 2015.

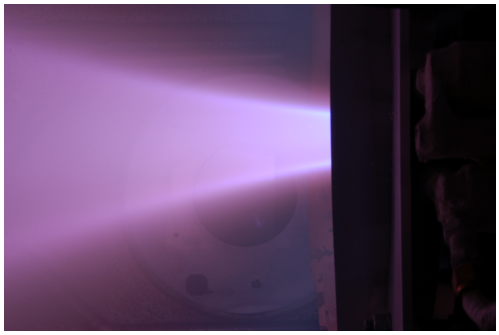

Figure 2 - The ALFA firing on September 12, 2017.

Thrust Generating Mechanisms

The LiLFA is a type of Applied-Field Magnetoplasmadynamic Thruster (AF-MPDT) using lithium as a propellant, as lithium has several advantages over more conventional propellants, such as xenon, krypton, or argon. Lithium has a lower first ionization potential (5.4 eV) than commonly used propellants (12.1 eV for xenon), which means more power can go to thrust generation instead of ionization. Additionally, it has a high second ionization potential compared to other propellants (75.6 eV compared to 21.0 for Xenon), reducing frozen flow losses. Lithium also has the benefit of reducing the work function of tungsten (the material from which the cathode is made) from 4.5 to 2.1 eV when barium is used as an additive, decreasing erosion and increasing the lifetime of our thruster.

The ALFA uses argon propellant, which is inferior to lithium for all of the reasons previously listed, but which has the advantage in the laboratory of being substantially less hazardous and time-consuming to perform tests with. This thruster is new to the laboratory as of 2017 and more details on it are given in "Current Research" below.

There are three primary mechanisms through which thrust is generated, each of which is outlined below.

1. Self-Field Component
   In the simplest configuration, MPDT's operate in what is known as the self-field mode, which is illustrated in Fig. 3. In this configuration, the thrust is generated by the cross product of the current travelling radially from the anode to the central cathode, and the magnetic field generated by that current travelling through the cathode, resulting in an axial force.

   While Self-Field MPDT's are simplest in design, they require MW levels of power, which are beyond the abilities of any present-day space-based power supplies. Application of an external magnetic field can reduce the power requirements, allowing operation in the 10s to 100s of kW. In the applied-field configuration, an additional thrust generating mechanism exists and is outlined in section 2.

   The self-field component of thrust has been shown to be $T_{SF} = bJ^2$, where J is the current through the electrodes and b is a geometric scaling factor.

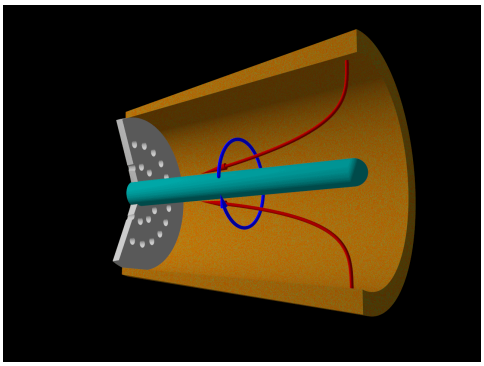

Figure 3 - Diagram of an SF-MPDT with an annular anode and central cathode. The current is shown in red, the magnetic field is blue, and the cross product of the two is purple.

2. Applied-Field Component

   The cross product of the current between the electrodes with an axial diverging magnetic field results in a force that acts to swirl the plasma. The mechanism by which this swirling motion generates thrust is an area of active research here at the EPPDyL. The general idea is that the swirling motion of the charged particles through the expanding magnetic field lines results in the conversion of kinetic energy perpendicular to the field lines into parallel kinetic energy because of adiabatic invariants.

   The applied-field component of thrust has been experimentally shown to be \(T_{AF} = kJB_Ar_a\), where \(k\) is a constant, \(B_A\) is the applied magnetic field strength, and \(r_a\) is the effective anode radius.

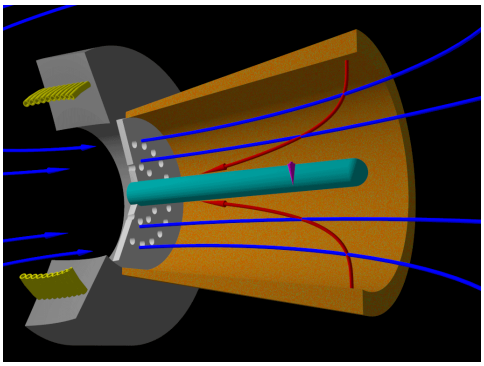

Figure 4 - Diagram of an AF-MPDT with an annular anode and central cathode. The applied magnetic field is generated by the solenoid wrapped around the thruster. The current is shown in red, the applied magnetic field is blue, and the cross product of the two is purple.

3. Cold Gas Component
   Because we are expanding a gas through a nozzle, there is also thrust generated that depends on our mass flow rate (\(\dot{m}\)), the gasdynamic pressure (\(P\)), and the area on which that pressure is pushing (\(A\)). The cold gas component of the thrust is then given by \(T_{CG} = c_s \dot{m} + PA\), where \(c_s\) is the speed of sound of the propellant.

Current Research

Research on the LiLFA is presently being conducted on the following topics:

- Dynamic resistance probe.
  A new probe, the Dynamic resistance probe (DRP), has been created and successfully tested for the first time (May 2015) to measure the deposition rate of lithium. Further testing will show if this probe is sensitive enough to measure deposition rates upstream of the thruster where propellant attachment to spacecraft is a concern.

- Thrust measurements.
  A new diagnostic for measuring thrust, isolating the component of force on the solenoid, has been incorporated into the existing thrust stand. This will help reveal the mechanism through which the applied-field generates thrust by providing a targeted measurement of the effective anode radius \(r_a\) described in the above section. The new thrust stand is illustrated in Figure 5.

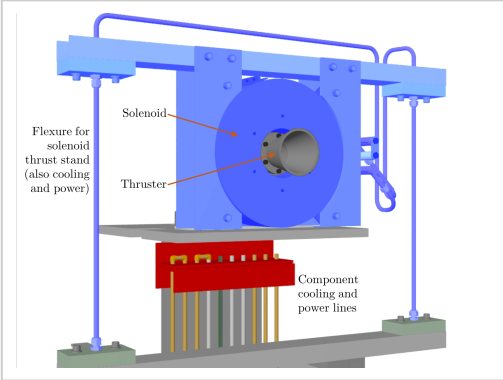

Figure 5 - Applied-field component thrust stand. All moving parts are shown in blue. As a force is exerted on the solenoid, the solenoid is deflected. This motion is measured and calibrated against a known force.

- ALFA.
  We have begun a testing campaign for the ALFA, which was constructed in the spring of 2017. Figure 6 shows the graphite anode, which is contoured to the magnetic field topology. Figure 7 provides a cutaway view of the assembled thruster. Figure 8 shows the thruster fully assembled.

Figure 6 - The graphite ALFA anode.

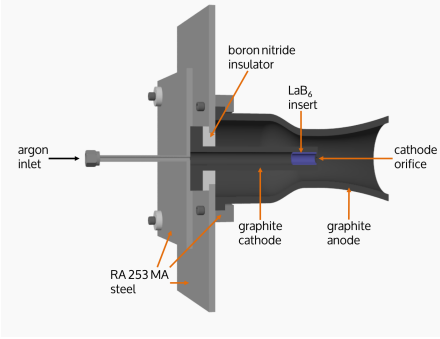

Figure 7 - Cutaway view of the ALFA.

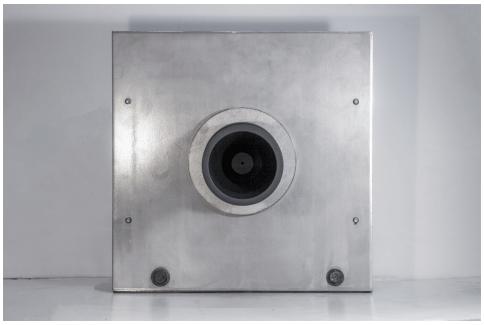

Figure 8 - The ALFA fully assembled.

Facilities

The EPPDyL is presently (2016) the only facility with an operating LiLFA. We currently have two LiLFA experimental models in our laboratory. The Open Heat Pipe LiLFA (OHP-LiLFA) designed and built by Thermacore Inc. and EPPDyL and, the workhorse of the present phase of our research, the 30kW MAI-LiLFA, designed and built at the Moscow Aviation Institute.

We fire the thrusters in a lithium-resistant steel vacuum chamber pictured in Figure 9. The chamber is actively cooled due to the high temperatures achieved during operation. The cooled walls also cause lithium to condense, and thereby help to maintain a low background pressure. We typically operate in the \(10^{-5}\) Torr regime with lithium and in the low \(10^{-4}\) Torr regime using argon. We achieve this pressure using the combination of a roughing pump, a roots blower, and a diffusion pump.

Figure 9 - Vacuum apparatus housing the LiLFA at the EPPDyL.

Lithium is loaded into the propellant reservoir using our glovebox, pictured in Figure 10, which is filled with argon to prevent any contamination of the lithium by reaction with the air.

Figure 10 - Glovebox for handling lithium.

We also possess the appropriate fire- and chemical-resistant clothing, as well as a supplied-air breathing system, for cleaning the contaminated chamber after firing with lithium. Some of this equipment is shown in use in Figure 11.

Figure 11 - Cleaning the vacuum chamber after firing the LiLFA.

LiLFA Publications

- Applied-Field Topology Effects on the Thrust of an MPDT (2017) (../publications/coogan-iepc-2017-182)
- A Critical Review of Thrust Models for Applied-Field Magnetoplasmadynamic Thrusters (2017) (../publications/coogan-jpc-2017-4723)
- A Graphite Orificed Hollow Cathode for an Argon Magnetoplasmadynamic Thruster (2017) (../publications/thesis/hollingsworth-thesis-2017)
- Extreme Environment Video Diagnostic for a Lithium Lorentz Force Accelerator (2017) (../publications/thesis/umansky_castro-thesis-2017)
- Direct Measurement of the Applied-Field Component of the Thrust of a Lithium Lorentz Force Accelerator (2016) (../publications/coogan-jpc-2016-4537)
- Liquid Metal Mass Flow Measurement by an Inductive Proximity Detector for Use in Conjunction with a JxB Pump (2016) (../publications/hepler-jpc-2016-4536)
- Control and Analysis of a JxB Pump Propellant Feed System for the Lithium Lorentz Force Accelerator (2016) (../publications/thesis/ilardi-thesis-2016)
- Dynamic Resistance Probe for the Measurement of the Mass Deposition Rate from a Condensible Propellant Thruster (2015) (../publications/coogan-iepc-2015-199)

- Design and Testing of a Propellant Feed System for the Lithium Lorentz Force Accelerator (2015) (../publications/thesis/mehl-thesis-2015)
- Investigation of Efficiency in Applied Field MagnetoPlasmaDynamic Thrusters (2012) (../publications/thesis/lev-thesis-2012.pdf)
- Scaling of Anode Sheath Voltage Fall with the Operational Parameters in Applied-Field MPD Thrusters (2011) (../publications/lev-iepc-2011-222)
- Scaling of Efficiency with Applied Magnetic Field in Magnetoplasmadynamic Thrusters (2010) (../publications/lev-jpc-2010-7024)
- A Critical Review of the State-of-the-Art in the Performance of Applied-field Magnetoplasmadynamic Thrusters (2006) (../publications/kodys-jpc-2005-4247)
- Lithium-Fed Arc Multichannel and Single-Channel Hollow Cathode: Experiment and Theory (2006) (../publications/thesis/cassady-thesis-2006)
- An Inverted-Pendulum Thrust Stand for High-Power Electric Thrusters (2006) (../publications/kodys-jpc-2006-4821)
- Investigation of Basic Processes in a Lithium Lorentz Force Accelerator through Plasma Flow Simulation (2005) (../publications/sankaran-pop-2005)
- Thermal Effects on Inverted Pendulum Thrust Stands for Steady-state High-power Plasma Thrusters (2003) (../publications/kodys-jpc-2003-4842)
- A Survey of Propulsion Options for Cargo and Piloted Missions to Mars (2003) (../publications/sankaran-icnta-2003)
- 3-D Characterization of the Plume of a Lithium Lorentz Force Accelerator (LiLFA) (2003) (../publications/thesis/kramer-thesis-2003)
- A Thrust Stand for High-power Steady-state Plasma Thrusters (2002) (../publications/cassady-jpc-2002-4118)
- Lithium Mass Flow Control for High Power Lorentz Force Accelerators (2001) (../publications/kodys-staif-2001)
- Thermal Analysis of a Lorentz Force Accelerator with an Open Lithium Heat Pipe (1999) (../publications/emsellem-iepc-1999-166)
- Lorentz Force Accelerator with an Open-ended Lithium Heat Pipe (1996) (../publications/choueiri-jpc-1996-2737)

Contact

Currently at Princeton:

- Will Coogan (../personnel#WillCoogan)

Former students:

- Mike Hepler
- Dan Lev
- Andrea Kodys
- Leonard Cassady
- Kamesh Sankaran

Former Visiting Researchers:

- Gregory Emsellem (Laboratoire de Physique des Milieux Ionisés)